
MODELING MULTI-AGENT MOTION DYNAMICS IN IMMERSIVE ROOMS

Mincong (Jerry) Huang and Stefan T. Radev

Department of Cognitive Science
Rensselaer Polytechnic Institute
Troy, New York, United States
`{huangm13, radevs}@rpi.edu`

ABSTRACT

Immersive rooms are increasingly popular augmented reality systems that support multi-agent interactions within a virtual world. However, despite extensive content creation and technological developments, insights about perceptually-driven social dynamics, such as the complex movement patterns during virtual world navigation, remain largely underexplored. Computational models of motion dynamics can help us understand the underlying mechanism of human interaction in immersive rooms and develop applications that better support spatially distributed interaction. In this work, we propose a new agent-based model of emergent human motion dynamics. The model represents human agents as simple spatial geometries in the room that relocate and reorient themselves based on the salient virtual spatial objects they approach. Agent motion is modeled as an interactive process combining external diffusion-driven influences from the environment with internal self-propelling interactions among agents. Further, we leverage simulation-based inference (SBI) to show that the governing parameters of motion patterns can be estimated from simple observables. Our results indicate that the model successfully captures action-related agent properties but exposes local non-identifiability linked to environmental awareness. We argue that our simulation-based approach paves the way for creating adaptive, responsive immersive rooms—spaces that adjust their interfaces and interactions based on human collective movement patterns and spatial attention.

Keywords Virtual Reality · Built Environment · Agent-Based Models · Simulation-Based Inference

1 Introduction

Spatial augmented reality is becoming increasingly commonplace and easier to integrate into the built environment. For example, immersive rooms, a type of virtual reality system evolved from the Cave Automatic Virtual Environment [CAVE; 1], can now support collocated and multi-user virtual world experiences. In some of the latest developments, the system consists of a room-scale panoramic visual display, a multi-channel spatial audio loudspeaker system, an overhead motion tracking system, and controllers that enable navigation and interaction within the virtual world [2, 3, Figure 1]. When multiple people reside in the immersive room, the extended virtual world provides a shared sense of auditory and visual immersion that people can freely experience within the room’s enclosure.

At the same time, spatial computing technologies have advanced significantly, expanding the scope and sophistication of interactive environments [4, 5]. As a result, immersive rooms now support a wide range of applications, including data visualization [6], situated learning [7], and life-size telepresence [8, 9], demonstrating their potential to reshape how people experience and inhabit built spaces. These capabilities are further extended by modern virtual environment platforms, such as game engines, which traditionally support head-mounted displays (HMDs). In HMD-based experiences, the virtual environment typically isolates an individual user from the physical world. In contrast, immersive rooms allow multiple users to share the same visual and auditory environment, supporting social interaction without obstructing sensory awareness of their co-present participants.



SYSTEM COMPONENTS

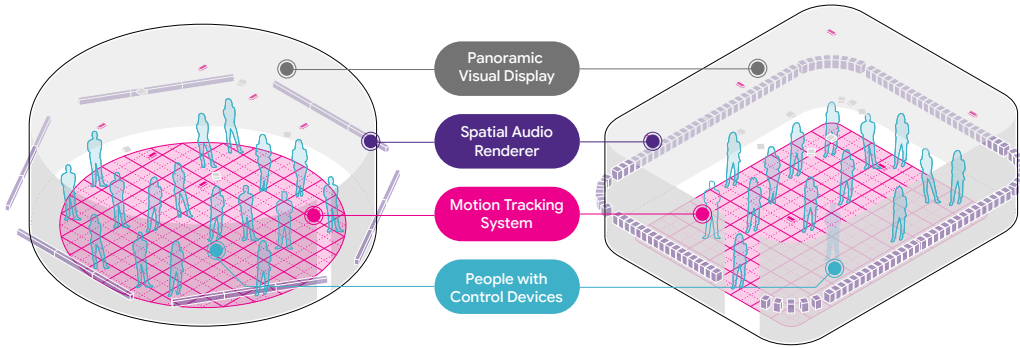


Figure 1: *Two examples of immersive rooms* [3]. These immersive rooms share common hardware components, with panoramic visual displays, spatially-situated speaker systems, and motion tracking systems. Both immersive rooms can host multiple agents, but they differ in terms of the spatial configuration of hardware components.

While spatial data on human movement in immersive rooms can be captured using built-in motion-tracking systems, such data can also be simulated within the virtual environment. Yet, due to the absence of comprehensive modeling frameworks, interpreting these data remains challenging. Most existing applications use motion data to enable interaction but implicitly assume that users will adapt to the technology. Consequently, they seldom leverage these data to infer behavioral patterns. Although tracking data can reveal motion dynamics at the individual level [10], such insights do not readily generalize to groups, limiting the development of robust human-centered interaction strategies.

Meanwhile, research on complex social dynamics has revealed a lot about how spatially-grounded perception of individual's surroundings shape collective self-organization as physical crowds [11]. Nevertheless, far less is known about how such dynamics unfolds when people engage with a shared built environment, even less so in the shared virtual world. From the perspective of interaction design, behavioral data offers critical information for shaping technologies that can accommodate human action and social engagement. In immersive rooms (or architectural environments more broadly) these data can illuminate the “activity space” for human-centered interaction design, especially in multi-user interaction settings [12, 13]. Accordingly, a formal modeling approach is necessary to draw connections between raw behavioral data and the higher-level spatial and social features that underpin the dynamics of human interactions.

In this work, we develop an agent-based model [ABM; 15–17] of perceptually-driven motion dynamics in immersive rooms. The rationale behind the model draws on a dynamical system perspective that frames the three-way relationship between the immersive room, its agents, and the extended environment. For a single human agent, the nervous system, the body, and the environment form a coupled dynamical system, from which agent action emerges and stabilizes through its internal states governing perception [14]. By analogy, if we consider the immersive room as a navigational “body” in the virtual world, the spatially distributed interaction between human agents within the room and the extended environment may be interpreted as an expression of the room’s internal state (see Figure 2). With this analogy as our working hypothesis, our secondary goal is to identify latent parameters from the time course of agents’ spatial movement in the immersive room. These parameters capture how agents process perceptual information about their virtual surroundings and respond both as individuals and as participants in a shared social context.

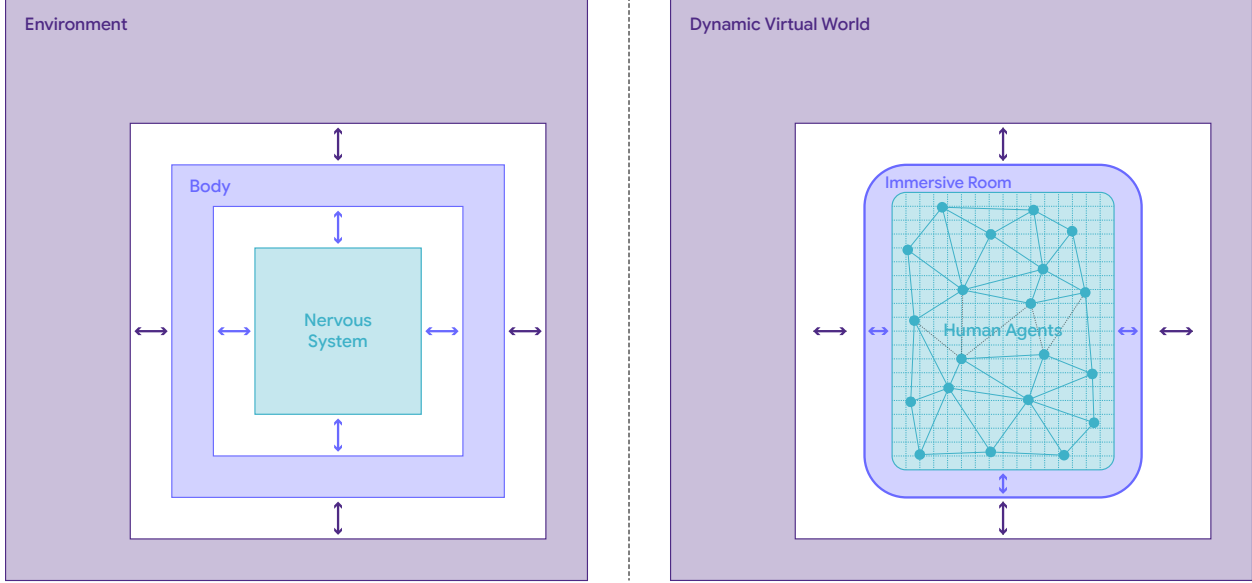


Figure 2: *Dynamical-system analogy of agent-environment interaction in immersive rooms.* Left: the original coupled-system perspective reproduced from [14]; right: the same perspective applied to immersive rooms, serving as the working hypothesis that interaction between human agents represents the internal state of immersive rooms in dynamic virtual environments.

The present study focuses on systematic model development and estimation within a simulated setting. From a technical standpoint, as the immersive room presents a novel context for computational modeling, simulation serves as a gateway to theory development, model instantiation, and knowledge discovery [18]. Accordingly, we employ simulation-based inference [SBI; 19], and more specifically amortized Bayesian inference [ABI; 20], to analyze human spatial data in a simulated immersive room. We combine an agent-based modeling (ABM) approach with diffusion models [DM; 21] of decision-making to simulate users' motion patterns in immersive environments, represented as time-series trajectories of virtual-world exploration. We then conduct a simulation and parameter recovery study using ABI to evaluate the identifiability of parameters governing agents' movement patterns and self-organization.

2 Background

As intrinsically motivated autonomous agents, humans in an immersive room can explore the virtual world independently or by following social cues. For instance, in a virtual museum with digital sculptures and paintings, an agent in the immersive room might approach an exhibit on the basis of their personal interest, or instead follow their peers to view an alternative display. As a result, their locomotion is shaped both via *global* interactions with their surrounding environments and *local* interactions with neighboring individuals. This setting has characteristics of agent-based systems, where global patterns emerge from local interactions. It also links to diffusion-based decision processes that are stimulus-driven and unconstrained by group-level dynamics. Both modeling approaches have well-established foundations in theory and computation. Below, we briefly review the relevant background literature and methods.

2.1 Agent-Based Models of Collective Motion Dynamics

Agent-based models (ABMs) describe emergent properties of self-motivated agents in an environment, capturing the spatiotemporal dynamics of their actions as a social system [15]. Agents in the environment follow local computational rules that subject them to the influence of their surrounding agents. This characteristic underscores the essence of collective motion dynamics in natural environments, from crowds [22] to bird flocks [23] to particles under the influence of force fields [24, 25].

ABMs have become a popular choice for high-fidelity computer simulations where behaviors of animal groups can be simulated *en masse* and rendered in early computer graphics [26]. In addition, ABMs have also been adopted in earlier works to simulate agent behaviors in architectural environments [27]. In these precedences, the agents are represented

as simple geometric abstractions, with their motion rule driven by real-time spatial information of their surrounding neighbors given limited sensing capabilities about the environment.

In ABMs, an agent's active perception involves sensing the surrounding neighbors as part of the environment. In collective motion, this perceptual coupling allows the agents to 1) align with their neighboring agents' instantaneous headings based on the difference in the available visual information between those who lead and those who follow [28, 29], and 2) maintain spatial cohesion by regulating their mutual distances for collision avoidance and movement sustenance [22, 30]. Stable simulation of motion patterns using ABMs require several foundational assumptions. First, the agents are modeled with shared internal properties, often with identical motion speeds and sensing capacities. Second, within the overall agent group, the agents are not self-guided, meaning that motion adjustments depend entirely on their spatial relationship with their immediate neighbors. Finally, the environment in which agents operate is treated as homogeneous, meaning that external influences are uniform across the agents.

For enhanced ecological validity, one or more of the above assumptions can be altered to introduce nuances to simulation. For instance, the agents can be equipped with a structured motion perception of the global environment, from which individual differences emerge from temporal variability in neighbor following and velocity changes [23]. Likewise, when agents operate in heterogeneous environments (i.e., an urban neighborhood with many landmarks), we can introduce variability to their local interaction rules, while the environment's global structure influences the agents' perception [31]. These cases illustrate the inherently hierarchical structure of ABMs, where agents can share global interaction properties while maintaining individual differences.

In our model, the virtual world only extends beyond the physical boundaries of immersive room. As a result, the room's interior is free of virtual contents and is treated as a homogeneous spatial environment for agent exploration. Agents interact locally with nearby neighbor, with their physical awareness determined solely by population density and rules of proxemics. Such configuration draws parallel with real-world pedestrians, wherein individuals can notice and respond to different points of interest in their surroundings. While the room's physical boundaries ultimately constrains where agents can move, the global navigation trajectory of the immersive room in the virtual world drives their motion, serving as a shared navigational substrate rather than an individualized frame of reference. This content sharing eliminates their tendency of staying at one place in the room, allowing them to interact with different neighbors over time.

2.2 Diffusion Process as Individual Motion Guidance

As suggested above, agents navigating in the immersive room can respond to salient spatial features in the extended virtual world. Thus, agent movement can be modeled primarily as a bottom-up, stimulus-driven process, where motor behaviors arise from online perception of dynamic auditory and visual cues [32, 33]. In this simplified environment, an agent's tendency to approach spatial objects depends solely on spatial relationships such as proximity and perceptual salience. Consequently, multi-agent motion emerges from vectors of self-guidance.

The perceptual motivation for the agents' movement in the immersive room can be derived from many driving factors in the extended virtual world, including motion onset [34], cross-modal interaction [35], and spatial tracking behaviors [36, 37]. The perception of moving spatial objects can influence the direction of people's movement. The influence depends on both the starting position and the direction of movement [38]. Similarly, moving auditory sources produce continuous perceptual streams that can guide head-orientation behaviors [39], which in turn influences head movement directions [40]. Beyond the mere presence of motion, spatial affordances such as distance [41], object salience [42], and temporal ordering [43] all shape an agent's motor response. Together, these factors drive agents to approach environmental objects of interest, a process reflected in their motion trajectories within the room.

In environments with multiple competing spatial stimuli, agents' independent perceptual decisions can be formalized using spatial variants of the diffusion model [DM; 21, 44]. The DM captures the time course of a decision-making agent's decisions under uncertainty; here, it can be extended in the context of spatial navigation, where an agent's initial position corresponds to a starting point, and the spatial objects it approaches serve as multidimensional decision boundaries. This extension naturally generalizes to social settings, where, under specific task constraints in the virtual world (e.g., foraging), the DM can serve as a parallel component of collective decision-making complementing the representation of individuals as reinforcement learning agents [45]. In contrast to reinforcement learning agents, however, our agents do not require explicit goals, and no reward structure is present. Instead, the DM serves to capture individual perceptual tendencies in the environment and introduce perturbation to the emergent collective motion.

2.3 Simulation-Based Inference

To connect the modeling approaches that bridge individual decision dynamics and collective motion behaviors, we need an inference framework that can recover the latent generative mechanisms from observed motion trajectories. To

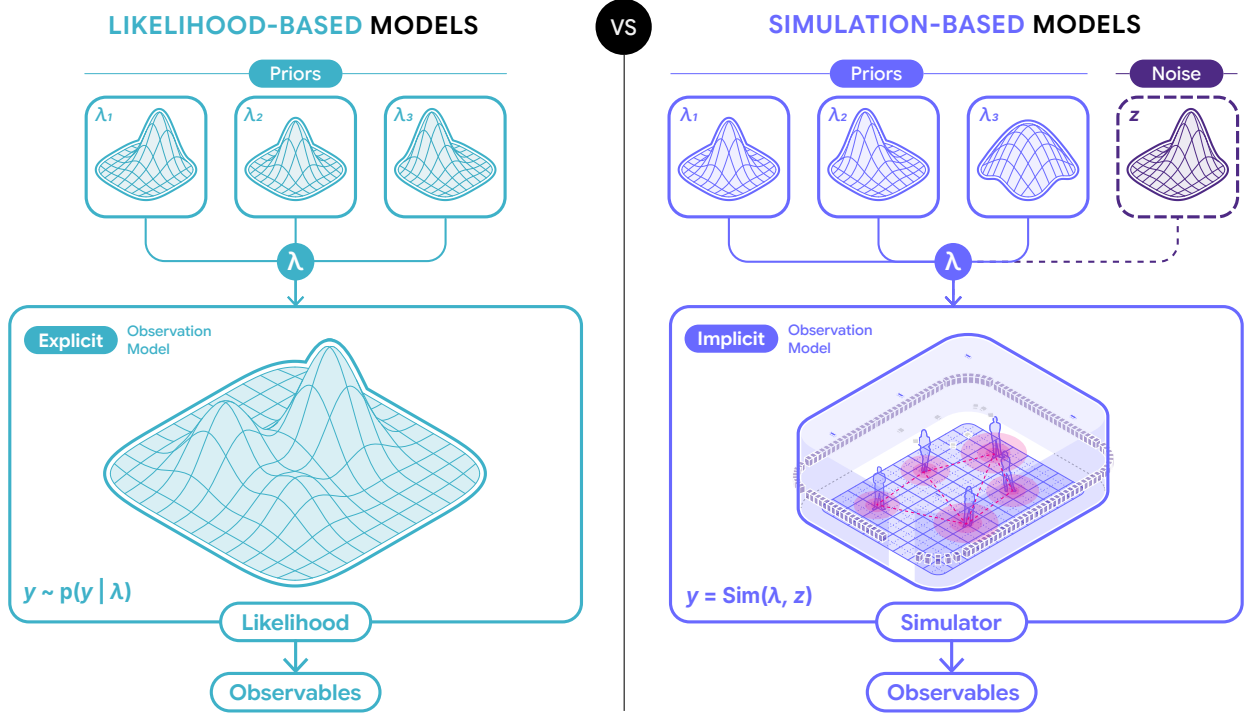


Figure 3: Flow diagram showing the distinction between likelihood-based and simulation-based generative models. In likelihood-based inference (left), the generative model is specified as a tractable probability distribution (e.g., Gaussian, Poisson, etc.). In simulation-based inference (right, this work), the generative model is specified as a set of computational rules or algorithmic steps which only implicitly define the distribution of observables y given input parameters λ .

this end, simulation-based inference (SBI) is a nascent family of statistical method for estimating the parameters of complex stochastic simulators [19]. In contrast to traditional statistical inference, where the observation model can be expressed as a known probability distribution (i.e., the likelihood), simulators are defined solely through computational or algorithmic rules (see also Figure 3). However, the ability to invert simulators (i.e., parameter estimation) can yield important insights into the system’s workings, which is why SBI can be an attractive tool for tackling ABMs.

Applications of SBI to ABMs have grown rapidly, spanning fields such as econometrics [46–48], competitive sports [49], and evolutionary biology [50]. Methodological advances have kept pace, including the development of surrogate models [51] and novel summary statistics [17, 52]. The push for data-driven approaches to ABMs within SBI arises from their distinct nature as simulation-first models, specifically, the complex interactions among agents that make parameter estimation difficult. Further complicating matters, simple agent rules can lead to complex emergent behaviors, making ABMs computationally surprising [53].

Model complexity places additional responsibility on researchers to encode appropriate assumptions about model parameters to ensure simulations are well-behaved. Complex formulations introduce many parameters to estimate, and researchers must carefully select constraints or prior distributions, as maintaining sensible simulation ranges often requires jointly adjusting multiple parameters. This makes results highly sensitive to priors on agent properties. In our case, introducing the spatial DM as a perturbation factor further tightens these conditions. These challenges make parameter estimation with ABMs extremely difficult for traditional methods [54].

A promising solution is amortized Bayesian inference (ABI), which uses synthetic data generated from arbitrary simulators to train a deep learning model for fully Bayesian [55] or point estimation [56]. ABI splits Bayesian estimation into a computationally intensive training phase and a cheap inference phase, allowing fast parameter estimation with real-world data, such as motion-tracking inputs. Moreover, ABI can accommodate the hierarchical structure of ABMs through its via multi-level neural network architectures [57]. This makes it an obvious candidate for studying parameter recoverability of agent motion patterns in immersive rooms.

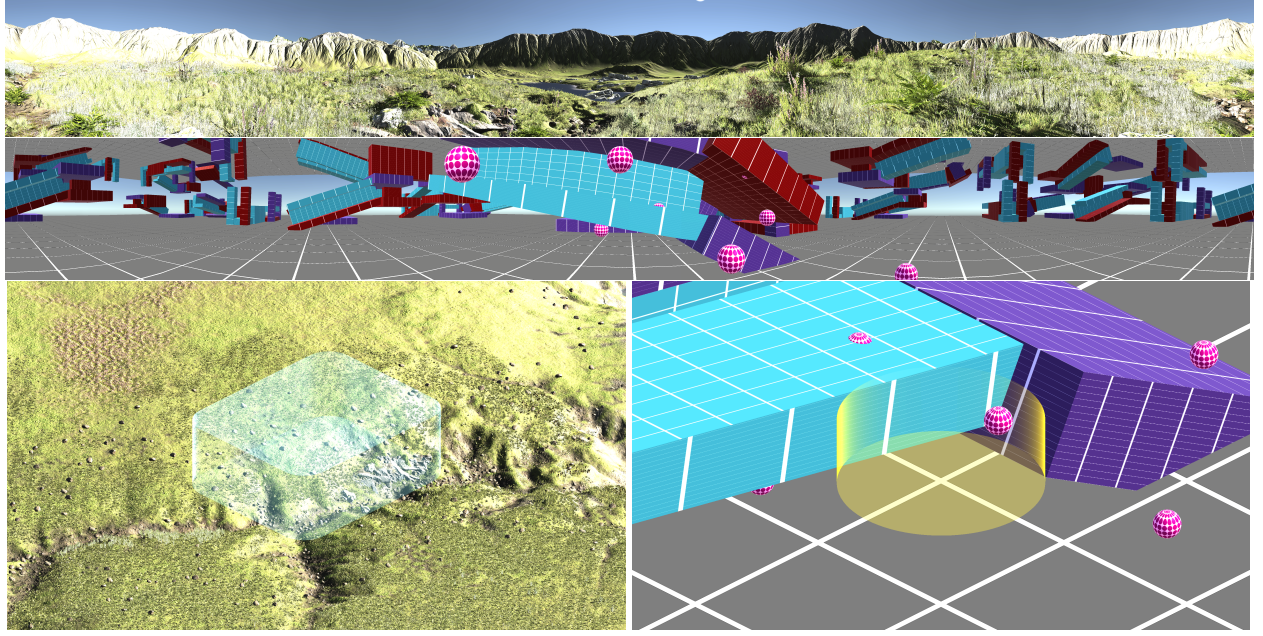


Figure 4: *Two examples of the environments set up for the development of our ABM. Top elongated:* a complex natural terrain with landscape features, offering a walkable experience populated with auditory beacons (e.g., birdsongs); *bottom elongated:* a geometric obstacle course for free-form drone navigation populated with visual beacons (e.g., spheres). The panoramic images are rendered using immersive rooms’ digital twins (bottom left, bottom right).

3 Methodology

3.1 Simulation Environments

Spatial beacons are contextually located multimodal stimuli in a navigational environment that anchor the spatial perception of human agents in immersive rooms. For instance, in a digitally reconstructed forest environment, spatial beacons can take the form of a large puffball mushroom on the forest floor or the song of a nearby cardinal. The concept of spatial beacons has applications in developing assistive technologies for real-world human navigation, specifically by incorporating multisensory information with geospatial data for cognitive map formation [58]. In the virtual world, we can taxonomize spatial beacons in at least three different categories: *visual beacons* as designated landmark that aims at agents’ body movements through viewing experience; *auditory beacons* as near-field virtual sound sources that trigger agents’ head movement through listening experience; *bimodal beacons*, which combine visual and auditory information to enhance perceptual salience and navigational guidance.

We constructed several test environments for navigable experiences that can be deployed in the immersive room. They include realistic scenarios, such as complex natural terrains with landscape features like mountains and lakes, to synthetic environments, such as geometric obstacle courses for free-form drone navigation (see Figure 4). At an abstract level, these environments share key properties: they provide spaces for free navigation within the room and spatial beacons distributed throughout. The use of game-based platforms in immersive rooms enables these beacons to be rendered in a spatially congruent manner. In general, we emphasize spatial rather than semantic congruence: for a bimodal beacon, we focus less on whether its audio and visual contents share meaning and more on whether they spatially coincide in the same location.

We simulate collective navigation using a digital twin of the immersive room in the virtual world [59]. At the most fundamental level, this digital twin is a modified first-person controller with a panoramic camera attached. In addition, the digital twin represents the spatial footprint of the immersive room in a 1:1 scale mapping to the virtual world, with human agents represented as a simple point with a 2D orientation and a defined sensing range for its neighbors. This set of representations allows the spatial information of the room and the agents to be projected onto the virtual environment. Conversely, as the room moves within the virtual world, positions and orientations of the spatial beacons are tracked by the agents relative to their egocentric reference frame.

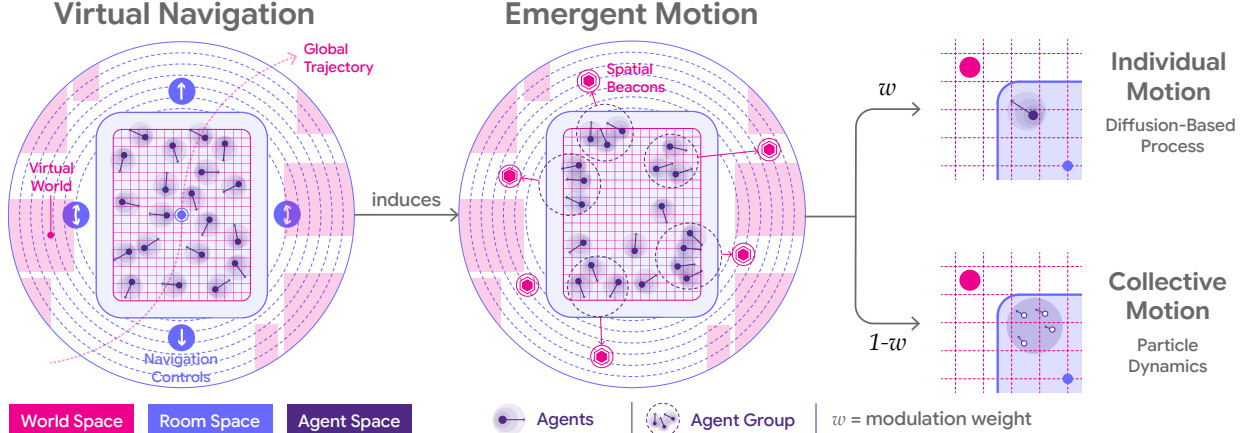


Figure 5: Conceptual diagram of our agent-based model (ABM) deployed in the immersive room. Motion perception during collective virtual navigation in the immersive room induces sensorimotor response to the virtual beacons. For motion patterns, individual (internal) influence is interpreted as a 2D drift diffusion process, whereas collective (external) influence is interpreted as a particle dynamic model. At a given point in time, a stationary weight w_k modulates the switch between internal and external influences. By extension, clustering of agents from the partitioned movement pattern can encode distributed spatial memory among the immersed human agent group.

As the room moves within the virtual world, the agents start perceiving and tracking the motion of its surrounding beacons [60, 61]. The agents act by moving and reorienting themselves without knowing beforehand which beacon to move and orient themselves to. The agents freely move within the room under this navigation scenario, where they may, for example, spontaneously take “mental notes” of the spatial objects that drive their curiosity. Different agents may be inclined to approach different beacons, and some agents may be more likely to follow suit with other agents than engage with the environments by themselves. This process combines individual and collective motion, producing emergent behavior as a collection of room-centered agent motion trajectories.

3.2 Model Formulation

The conceptual illustration of our motion dynamics model is shown in Figure 5. As discussed in Section 2, the agents’ emergent motion pattern is activated by the individual motion-induced response to the virtual navigation process of the immersive room in the virtual world. Therefore, we formally define *external influence* as agents’ tendency to be directed to a spatial beacon, a proxy representation of their active perception; and *internal influence* as the agents’ inclination to move along with their surrounding neighbors.

For each agent $a = 1, \dots, A$ moving within a room M bounded by Ω_M , we represent the physical aspect of collective motion of all agents by their positions $\mathbf{X} = (\mathbf{x}_1, \dots, \mathbf{x}_A)$ and orientations $\Theta = (\theta_1, \dots, \theta_A)$. In addition, we also collect the individual agents’ number of neighbors $N = (N_1, \dots, N_A)$ as well as the average neighbor distances $\mathbf{D} = (D_1, \dots, D_A)$. Using the immersive room’s digital twin, an agent a in the room would collectively navigate through a virtual world that is populated with multiple spatial beacons, $b = 1, \dots, B$, along with their neighbors in the same room, $n = 1, \dots, N$. We consider the agents’ locomotion and reorientation as parallel events with separate action states. In other words, the agents can move and rotate in both concurrent and parallel fashions. It is possible for the agents to approach a beacon without reorientation, or simply reorient themselves without moving. Table 1 summarizes the notation used for formulating the model.

We formulate an agent a ’s motion dynamics as a modulation between external and internal influences, namely,

$$\theta_{a,t} = w_a \theta_{a|b,t} + (1 - w_a) \theta_{a|n,t} \quad (1)$$

$$\mathbf{x}_{a,t} = w_a \mathbf{x}_{a|b,t} + (1 - w_a) \mathbf{x}_{a|n,t}, \quad (2)$$

where a ’s influences at time t are given by their change in orientation $\theta_{a,t}$ as well as their change in position $\mathbf{x}_{a,t}$. The agent’s external influence, denoted as $\theta_{a|b,t}$ and $\mathbf{x}_{a|b,t}$ ¹, is given by its approached beacon; by contrast, its internal influence, denoted as $\theta_{a|n,t}$ and $\mathbf{x}_{a|n,t}$, is given by its surrounding neighbors. While $\theta_{a|b,t}$ and $\mathbf{x}_{a|b,t}$ are updated through a spatial diffusion-based model with the agent a ’s positions of approached beacon as decision boundary, $\theta_{a|n,t}$ and

¹One should read $a|b$ as “agent a given beacon b ” or “agent a as influenced by beacon b .”

Table 1: Symbols and notation for the proposed agent-based motion of emergent human motion in immersive rooms.

Notation	Meaning
<i>Indices</i>	
$a = 1, \dots, A$	Indices of A agents
$b = 1, \dots, B$	Indices of B beacons
$n = 1, \dots, N$	Indices of N neighboring agents
<i>Positions</i>	
$\mathbf{x} = (\mathbf{x}_1, \dots, \mathbf{x}_a, \dots, \mathbf{x}_A)$	The set of positions for all agents
$\mathbf{x}_a = (x_a, y_a)$	Room-centered position of an agent a
$\mathbf{x}_i = (x_n, y_n)$	Room-centered position of a neighboring agent i
$\mathbf{x}_b = (x_b, y_b)$	Room-centered position of a spatial beacon j
$\mathbf{x}_M = (x_M, y_M)$	World-centered position of the room M
$\mathbf{x}_{a b}$	Position of agent a as influenced by a spatial beacon b
$\mathbf{x}_{a n}$	Position of agent a as influenced by a neighboring agent n
<i>Orientations</i>	
$\theta_{a b}$	Orientation of agent a as influenced by a spatial beacon b
$\theta_{a n}$	Orientation of agent a as influenced by a neighboring agent n
<i>Agent properties</i>	
w_a	External influence weight for an agent a
r_a	Neighbor sensing range of an agent a
v_a	Locomotive drift rate of an agent a
ω_a	Rotational drift rate of an agent a
σ_a	Diffusion coefficient for the position noise of agent a
η_a	Rotational noise variance of agent a
<i>Observables</i>	
$\mathbf{X} = (\mathbf{x}_1, \dots, \mathbf{x}_A)$	Positions for all agents
$\Theta = (\theta_1, \dots, \theta_A)$	Rotations for all agents
$\mathbf{N} = (N_1, \dots, N_A)$	Number of neighbors for all agents
$\mathbf{D} = (D_1, \dots, D_A)$	Average distances of neighbors for all agents
<i>Other properties</i>	
Ω_M	Boundary of the room M
R_M	Beacon detection range for the room M

$\mathbf{x}_{a|n,t}$ are updated through an ABM of self-propelling particle dynamics. All influences are specified in 2D, following both the sensing capability of the motion tracking system and the rendering capability of the multi-channel spatial audio speaker system².

A visual breakdown of the influences can be found in Figure 6. Below, we formulate the components of these influences in greater detail.

3.3 External Influence: Individual Motion as Spatial Drift Diffusion

We use a spatial diffusion model in 2D space to provide a baseline representation of the agent's external influence. As the room travels in the virtual world, it detects a subset of spatial beacons within its detection range R_M , where $\|\mathbf{x}_b - \mathbf{x}_M\| < R_M$. Within this subset of beacons, the agents approach the one that is closest to them, namely:

$$b_{a,t} = \arg \min_{b \in B} \|\mathbf{x}_{a,t} - \mathbf{x}_{b,t}\|, \quad (3)$$

so that, within the room's boundary Ω_M , agent a approaches b_a based on b_a 's relative position in the agent-centered coordinates $\mathbf{x}_{a,b} = \mathbf{x}_b - \mathbf{x}_a$, as well as the relative orientation, $\theta_{b|a} = \mathbf{x}_{a,b} - \theta_{a|b,t}$. The orientation update for the agent a can be expressed as

$$d\theta_{a|b,t} = (\omega_a + \phi_{a,t})dt, \quad (4)$$

where $\omega_a = \tan^{-1}(\mathbf{x}_{a,b})$ is the rotational drift rate (speed) of the agent a , and $\phi_{a,t} \sim \mathcal{U}(-\kappa_a, \kappa_a)$ is a non-cumulative rotational noise component that follows a uniform distribution, where $\kappa_a < 0.01$ controls the variability of the agent's

²The spatial sound sources are typically rendered in the virtual world using wave field synthesis [62].

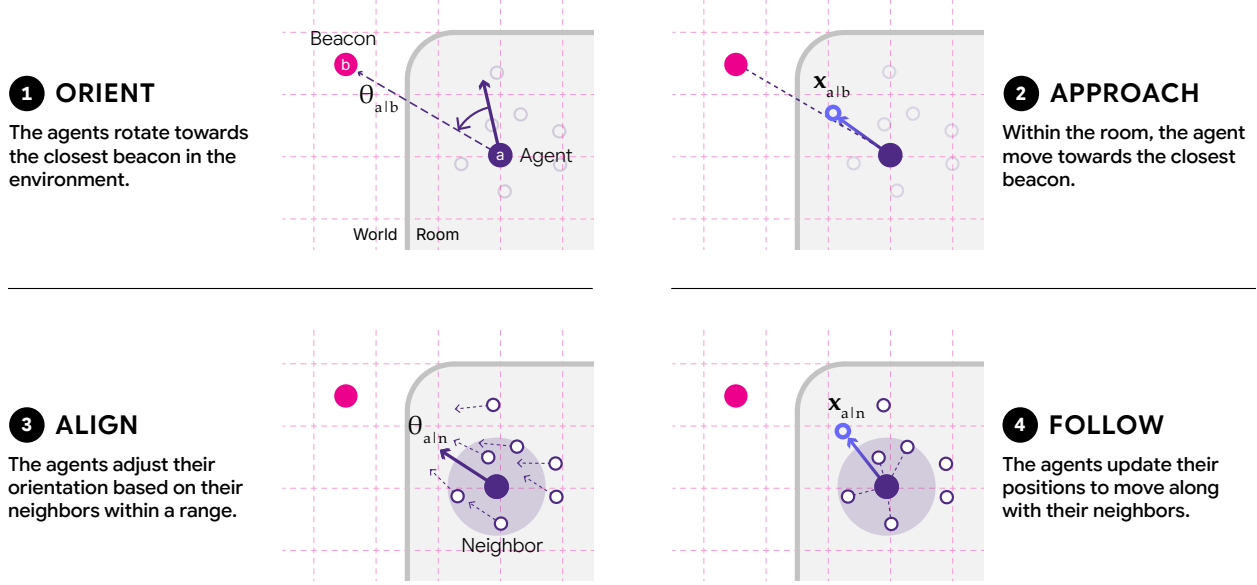


Figure 6: *Influence vectors driving agent motion in an immersive room.* These influence vectors are separated into external (individual, top half) and internal (collective, bottom half) components, each exhibiting separate rotational (left half) and translational (right half) motion. The gray boundary and gray area represents the immersive room’s spatial footprint, the solid purple dot represents an agent a of focus, the white circle dots depict neighboring agents (within the shaded purple circle), and the solid magenta dot represents a spatial beacon. Individual orientation and approach to the spatial beacon both follow a diffusion model in 2D (external influence), whereas collective (internal) alignment and following influences conform to a Vicsek model.

reorientation at each time step. In addition, the positional update for the agent a can be expressed as:

$$d\mathbf{x}_{a|b,t} = v_{a,t} \begin{bmatrix} \cos \theta_{a|b,t} \\ \sin \theta_{a|b,t} \end{bmatrix} dt + \sigma_{a|b} d\mathbf{W}_t, \quad (5)$$

where \mathbf{W}_t is a two-dimensional Wiener process, and $\sigma_{a|b} > 0$ controls the diffusion amplitude (i.e., the scale of positional noise). The scalar $v_{a,t}$ denotes the instantaneous speed (drift magnitude) of agent a , and the unit vector $[\cos \theta_{a|b,t}, \sin \theta_{a|b,t}]^\top$ specifies its current heading relative to the beacon b . This means that, at each time step, the agent a moves approximately in the direction of the beacon b with adjustment to noise perturbation. The drift magnitude v may vary between agents and between simulations, and therefore becomes a candidate parameter to capture the influence of the virtual world on the agents.

3.4 Internal Influence: Collective Motion as Active Particle Dynamics

To express collective motion, we follow the Vicsek model [24] as our baseline formulation of internal influence. The Vicsek model is an ABM that considers the alignment dynamics of individual agents and their local interaction with neighborhood agents, where the agent a takes into account the average orientation of neighboring agents $n = 1, \dots, N$ under a sensing radius r_a , and adjust its orientation $\theta_{a|n,t}$ accordingly. We can formalize the angular update for the internal influence of agent a as

$$\theta_{a|n,t} = \langle \theta_{n,t} \rangle_{||\mathbf{x}_{a,t} - \mathbf{x}_{n,t}|| < r_a, n \in N_t} + \gamma_{a,t}, \quad (6)$$

where θ_a, θ_n are the orientations of agent a and their neighbor n within a sensing distance r_a , $\langle \theta_n \rangle$ denotes the average of all neighbor orientations within the agent’s sensing radius, and $\gamma_a \sim \mathcal{N}(0, \eta_a)$ represents rotational noise for agent a under variance η_a . Both r_a and η_a may vary between agents and between simulations, and therefore are candidate parameters that capture the agents’ local rules in the immersive room. The motion update under internal influence is expressed as:

$$d\mathbf{x}_{a|n,t} = v_{a,t} \begin{bmatrix} \cos \theta_{a|n,t} \\ \sin \theta_{a|n,t} \end{bmatrix} dt, \quad (7)$$

where $\mathbf{x}_a, \mathbf{x}_n$ are the orientations of agent a and their neighbor n within a sensing distance r_a , and $\langle \mathbf{x}_i \rangle$ denotes the average of all neighbor positions. The sensing distance r_a for alignment and cohesion dynamics are identical since the number of agents is finite and the interaction boundary is finite and non-periodic.

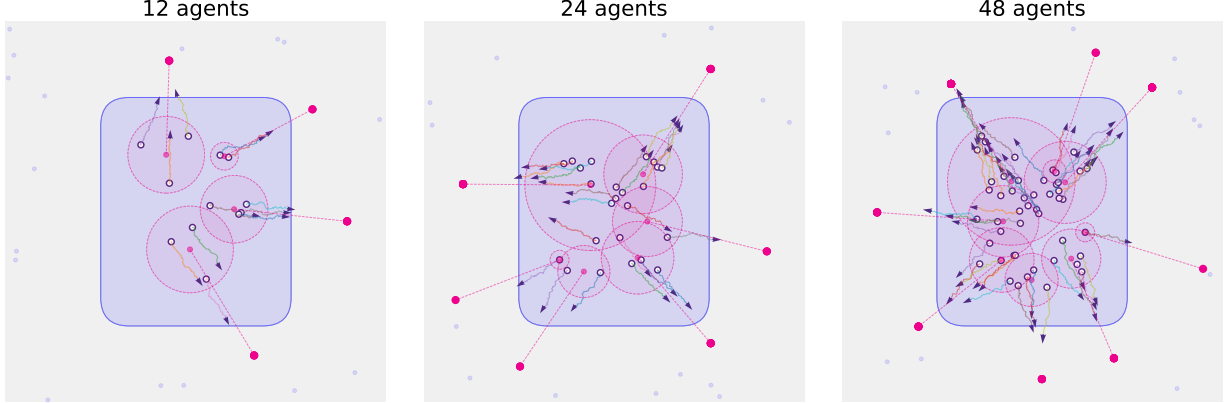


Figure 7: Simulated onset trajectories for three different agent and beacon configurations. The blue-shaded rectangle represents the immersive room’s spatial footprint in the virtual world, surrounded by beacons that are either approached (magenta dots) or not approached (blue dots) by different agents in the room (white circle dots with colored paths). Each beacon has a cluster of agents approaching it (magenta dashed circles).

4 Implementation

4.1 Forward Model and Simulation

The forward model detailed in Section 3 is implemented in two ways. First, a playable interactive simulator visualizing the real-time motion dynamics is implemented using the Unity game engine and integrated as part of the digital twin [59]. This simulator assumes an infinite time horizon, where a switching regime between beacons is incorporated for the agents to update the beacon to approach.

To generate our training data for the neural estimator, the same simulator is also implemented in Python assuming a finite time horizon without a switching regime. We use a baseline configuration of $A = 49$ agents in the same room and $B = 8$ beacons within its sensing range traveling in $T = 600$ time steps with time resolution $dt = 0.1$, lasting for 60 seconds in records. Example visualization for simulation onset can be found in Figure 7. This baseline configuration is closely aligned with the real-world infrastructural capability for the same task design. The observables for the simulator is a collection of agent time series, including their positions $\mathbf{X} = (\mathbf{x}_1, \dots, \mathbf{x}_A)$, rotations $\Theta = (\theta_1, \dots, \theta_A)$, the number of neighbors $\mathbf{N} = (N_1, \dots, N_A)$, and average neighbor distances $\mathbf{D} = (D_1, \dots, D_A)$. For data augmentation, we also compute the angular velocity from Θ and the change in neighbor count from \mathbf{D} . In both simulators, we confine the agents to the room’s spatial boundary Ω_M , so that they realistically reflect the real-world experience of the immersive rooms.

4.2 Prior Specification

We are interested in estimating four key parameters: the influence weight w , sensing radius r , movement speed v , and internal noise variance η . These parameters jointly describe the agent’s action capability and environmental awareness. The model can be implemented with different degrees of parameter sharing: *no pooling* (each agent has distinct parameters), *complete pooling* (all agents share the same parameters), or *partial pooling* (hierarchical structure capturing individual deviations from global means). In this proof-of-concept study, we use complete pooling with the following priors:

$$w \sim \text{Beta}(2, 2), \quad r \sim \text{LogNormal}(0, 0.5), \quad \eta \sim \text{Beta}(2, 5), \quad v \sim \text{Beta}(2, 2). \quad (8)$$

However, we recommend partial pooling for heterogeneous real-world data [63].

4.3 Neural Estimator for Simulation-Based Inference

Our neural estimator, design with the BayesFlow library for amortized SBI [20], is used to perform posterior estimation of the model parameters specified in Section 4.2. A schematic diagram of the neural estimator and its relationship with the simulated data can be found in Figure 8.

Given the simulated trajectories of agent positions, orientations, adjacent neighbor counts, and average neighbor distances as inputs, the summary network consists of two 1D-convolutional layers for filtering, followed by a long

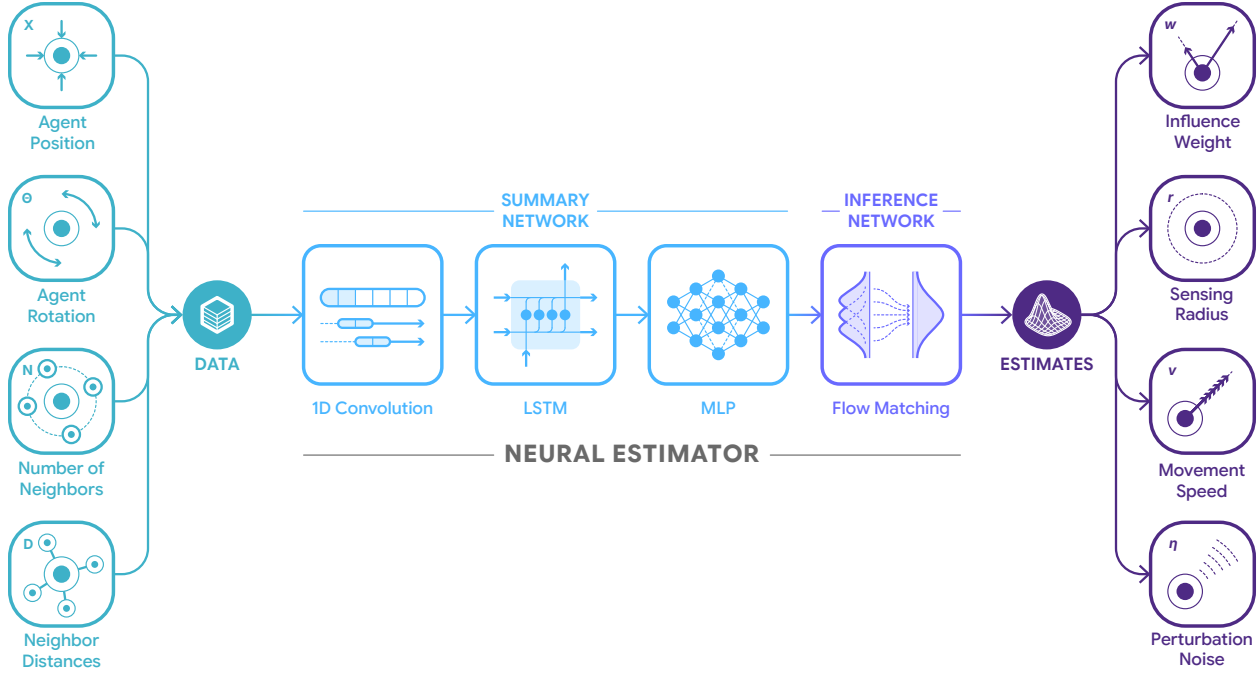


Figure 8: *Schematic diagram of our SBI workflow.* The agent data, which consists of position, rotation, adjacent neighbor counts, and average neighbor distances, is used to train a two-stage neural network architecture with 1) a summary network that includes 1D convolution filtering layers, agent-level embeddings through a Long Short-Term Memory (LSTM) network, and a fully-connected dense layer, and 2) a flow matching inference network [64]. The inference network estimates four target parameters: influence weight w , sensing radius r , movement speed v , and perturbation noise η .

short-term memory (LSTM) network as agent-level embedding. The embedded data is obtained by passing the LSTM to a fully-connected dense neural network layer.

For parameter estimation, the embedded data needs to be passed through an inference network that can estimate the parameter posterior $p(w, r, \eta, v | \mathbf{X}, \Theta, \mathbf{N}, \mathbf{D})$. We choose flow matching [64] as a flexible and lightweight generative architecture. To evaluate parameter recoverability as a function of the simulation budget, we generate training sets with $B \in \{3,000, 30,000\}$ simulations. For each of the simulation budgets, we train a neural estimator for 100 epochs with a batch size of 32 and assess parameter recoverability on $S = 300$ unseen simulations.

5 Simulation Study

To assess the global performance of our neural estimator as part of the SBI workflow, we validate the model from two different perspectives. First, we use simulation-based calibration [SBC; 65, 66] to inspect the computational faithfulness of the estimator. Then, we evaluate whether agents' latent properties (i.e., parameters) can be recovered under idealized conditions by assessing parameter recovery. We provide both graphical checks and numerical summaries of these results.

5.1 Computational Faithfulness: Testing Calibration

First, we check whether the approximate posteriors are properly calibrated, that is, whether they faithfully reflect the epistemic uncertainty of the estimation problem. We leverage SBC, which evaluates properties of an ensemble of posteriors estimated from simulated data relative to the prior. Here, we evaluate the empirical coverage of credible intervals obtained from posterior samples, rather than relying on the more common inspection of ranks or other sophisticated diagnostics [67]. Since any proper posterior has correct coverage under the true model, any deviation from the ideal coverage indicates approximation problems. The empirical coverage $c(\alpha)$ of a credible interval of size α

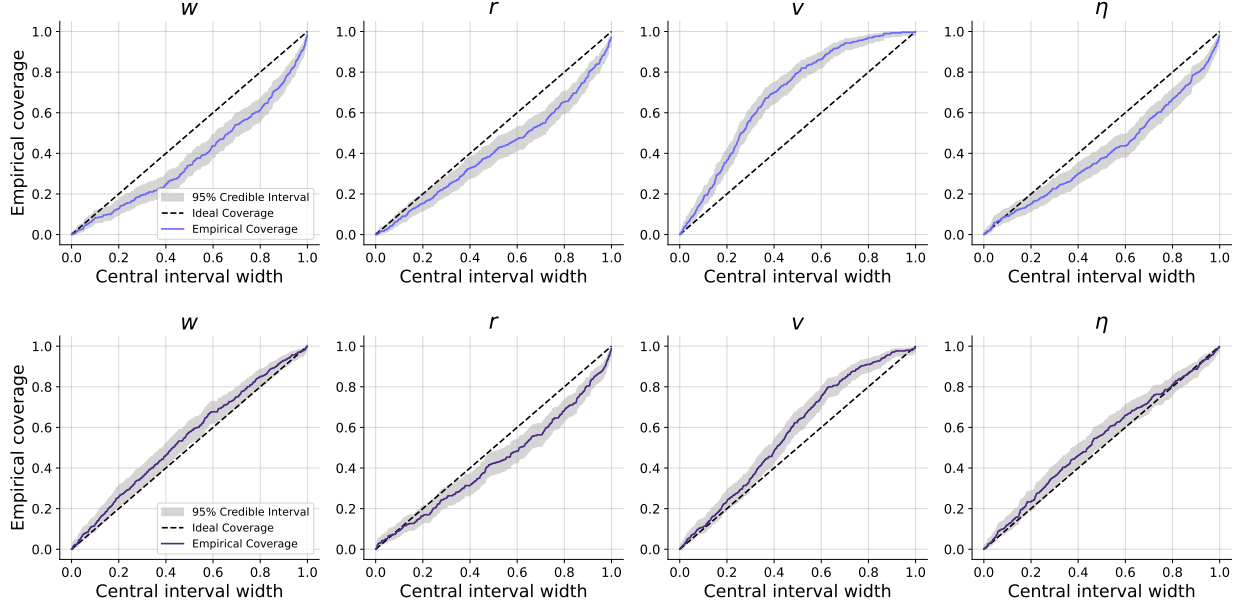


Figure 9: *Empirical coverage for the two simulation settings with different number of simulations as an indicator of computational faithfulness.* Top: coverage of the neural estimator trained on 3,000 model simulations. Bottom: coverage of the neural estimator trained on 30,000 simulations.

(e.g., $\alpha = 0.95$) is computed from S test simulations and corresponding posterior samples

$$c(\alpha) = \frac{1}{S} \sum_{s=1}^S \mathbf{1}[\lambda_s \in [q_{s,\beta}, q_{s,1-\beta}]], \quad (9)$$

where $\mathbf{1}$ is the indicator function, $\beta = (1 - \alpha)/2$ and $1 - \beta$ define the bounds of the credibility interval, and $q_{s,\beta}$ is the β -quantile derived from the posterior samples $\{\hat{\lambda}_s\}$ of the s -th test simulation.

Coverage can be checked graphically (Figure 9) or summarized via the Expected Calibration Error (ECE) metric for a range of widths α_k :

$$\text{ECE} = \frac{1}{K} \sum_{i=1}^K |c(\alpha_k) - \alpha_k|. \quad (10)$$

The parameter-wise empirical coverage of our neural estimator is shown in Figure 9, and the parameter-wise ECE is provided in Figure 5.2. From the diagnostics, we observe that the model is generally well-calibrated for the estimation of w , r , and η , but is overly confident when estimating v . This is most evident in the coverage plots, where the ideal coverage (black dashed line) for well-calibrated parameters falls within the 95% credible intervals of the empirical coverage curve, while for v , the coverage lies mostly above the ideal. A similar pattern is seen in the ECE, where v shows a significant increase. Calibration also improves with increased size of training set. These results suggest that the neural estimator is too certain when estimating v , but otherwise reproduces the prior distribution well for the other parameters.

5.2 Model Sensitivity: Testing Parameter Recovery

Next, we assess the global inferential adequacy of the neural estimator—how well it can recover model parameters from observable quantities. We compare the estimated posteriors to the true simulator parameters to evaluate both accuracy and confidence. Specifically, we quantify parameter recovery error and posterior contraction (uncertainty reduction relative to the prior) as summary measures of inferential performance.

Similar to empirical coverage, parameter recovery can be inspected graphically (Figure 10). Effective parameter recovery is characterized by posterior distributions centered around the true parameters with reduced variance relative to prior distributions. As a summary metric, we also compute the Pearson correlation coefficients r between the

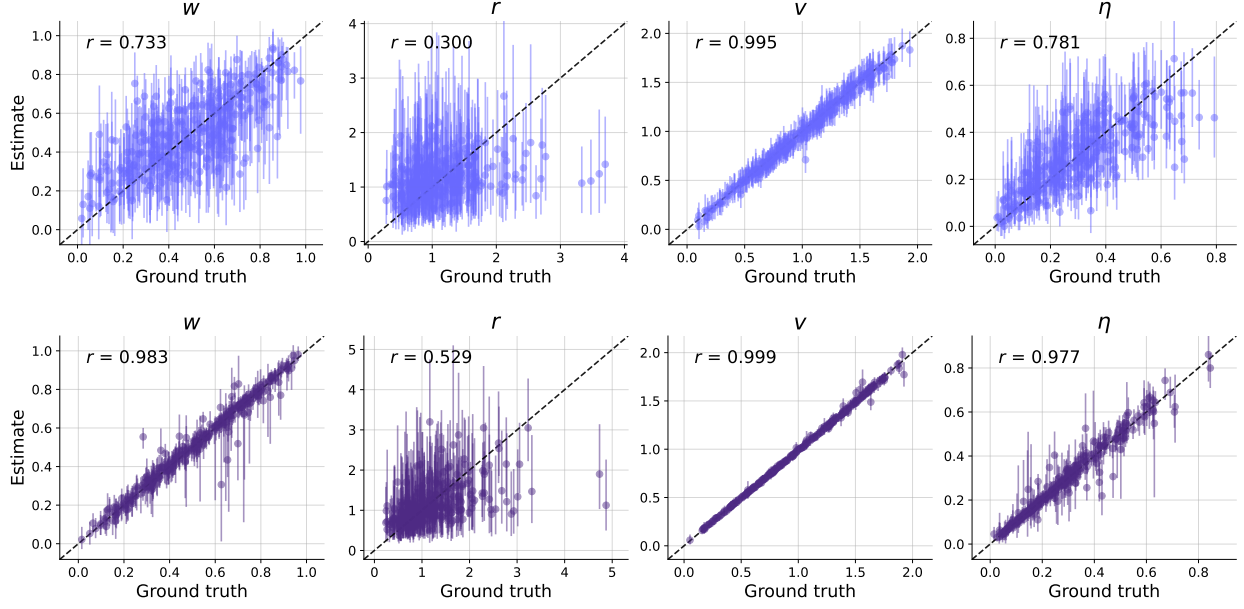


Figure 10: *Parameter recovery for two simulation budgets.* Top: recovery from the neural estimator trained on 3,000 simulations. Bottom: recovery from the neural estimator trained on 30,000 simulations. Dots indicate posterior medians and vertical lines denote 95% credible intervals.

Table 2: Parameter recovery metrics across two simulation budgets.

Metric	Training Set $N = 3,000$				Training Set $N = 30,000$			
	w	r	v	η	w	r	v	η
Calibration Error	0.085	0.077	0.207	0.015	0.013	0.079	0.070	0.021
NRMSE	0.209	0.192	0.063	0.187	0.080	0.150	0.019	0.073
Posterior Contraction	0.719	0.585	0.964	0.675	0.969	0.729	0.997	0.974

ground-truth simulator parameter and the median posterior estimates produced by the neural estimator, with better performance indexed by higher correlations.

The uncertainty of the neural estimator can be quantified through posterior contraction, which measures how much the posterior distribution narrows around the true parameter as more data become available. Greater contraction indicates improved estimator performance and a more information gained. Formally, posterior contraction (PC) is defined as

$$PC = 1 - \frac{\text{Var}(\lambda_i^{\text{post}})}{\text{Var}(\lambda_i^{\text{prior}})}, \quad (11)$$

where $\text{Var}(\lambda_i^{\text{post}})$ is the posterior variance and $\text{Var}(\lambda_i^{\text{prior}})$ is the prior variance [68]. The total PC is the average of (11) across S test simulations. For completeness, we also compute the Bayesian normalized root-mean-square error (NRMSE), given by

$$\text{NRMSE} = \frac{1}{\lambda_{\max} - \lambda_{\min}} \sqrt{\frac{1}{S} \sum_{s=1}^S \frac{1}{J} \sum_{j=1}^J (\hat{\lambda}_{j,s} - \lambda_s)^2}, \quad (12)$$

where λ_s is the ground-truth parameter, λ_{\max} and λ_{\min} are the maximum and minimum parameter values, and $\hat{\lambda}_{j,s}$ is the j -th posterior sample obtained for the s -th simulation. Together, these measures indicate whether something about the model parameters can be learned under idealized conditions (i.e., *in silico*).

The parameter-wise results for recovery are shown in Figure 10, and the parameter-wise PC and NRMSE are summarized in Figure 5.2. We observe that the model can recover w , v , and η , but is limited in its recovery of r . This is apparent in graphical inspection of recovery, where uncertainty most notably reduced for v , followed by w and η . Recovery of

these parameters improves when more simulations are available, a typical behavior of SBI methods [69]. Single-valued metrics also confirm this observation, where we observe higher PC and lower NRMSE for w , r , and η , while the information gain for r remains limited. These results suggest that the neural estimator can detect local non-identifiability of r , but is otherwise capable of identifying most model parameters based on the simulated data.

6 Discussion

In this work, we presented a novel computational model of human motion dynamics during collective navigation of virtual worlds in immersive rooms. At a high level, the model combines a diffusion-based and agent-based modeling approaches to represent individual agents' influences as spatial cognition and social dynamics, where collective motion patterns emerge from the agents' volitional interaction with the virtual world. The immersive room setting, in which the same virtual world experience is shared by multiple agents in the physical world, allows us to situate these influences and contain their observations in a unified manner, thereby highlighting the use of new tools to generate novel concepts and models of human interaction.

Further, we leveraged neural simulation-based inference (SBI), where we use a neural estimator to assess how well agents' internal properties can be identified from their observable motion patterns. As our results suggested, the agents' exploration dynamics during virtual navigation, captured by the tradeoff between individual agency and the tendency to "go with the flow", can be characterized by the neural estimator with reasonable accuracy. In particular, parameters directly linked to an agent's actions (i.e., the modulation weight w and motion speed v) were recovered reliably, and remain sensitive under perturbative conditions, as manifested by the neural estimator's high performance in recovering the agent's rotational noise variance η . In addition, the neural estimator also detects the limited identifiability of the parameter reflecting agents' local environmental awareness (i.e., sensing radius r).

Among the identifiable parameters, the agent's modulation weight w , which can be interpreted as a state of the agent's motion governed by its situational awareness, is recovered with greater uncertainty than the drift rate v . This uncertainty is similar to that observed in the recovery of η , which reflects the decision uncertainty for the individual agent under internal influences. In other experiments, we observe that fixing noise variance η resulted in poorer estimation of the modulation weight w . This suggests some degrees of interaction between the parameters. We interpret this as the result of a mixture effect introduced by the combined influences. In real-world scenarios, agents may not explicitly consider how much they wish to explore independently versus follow others. They are likely agnostic to both approaches and may lean toward one or the other without being self-aware. The same uncertainty can also be explained in data space: when the agent balances the two influences, the resulting data become ambiguous from the perspective of each isolated influence. This compounded ambiguity likely contributes to the variability in the estimated modulation weights.

The auditability of our SBI framework is afforded by the extensive diagnostics inherent in Bayesian workflows [70] and made efficient through amortization. As demonstrated in our work, ABI can not only recover the governing parameters explicitly related to the agent's actions, but also detect the non-identifiability of model parameters related to the agents' local awareness of the environment. ABI's effectiveness in the context of this work has a broader implication to the use of immersive room as a tool to study perceptually-driven spatial cognition. On the one hand, we see an increasing adoption of room-scale virtual reality system with spatial audio capabilities in the study of multimodal perception [71, 72]. On the other hand, from the perspective of modeling, the use of diffusion-based approaches in modeling perceptually-driven dynamics of cognition, especially those involving auditory perception, is also a relatively recent [73]. By integrating our model in a tool-driven setup, we reveal the potential to make these two trends converge by developing structured theories of perceptually-driven spatial cognition in multi-user virtual environments.

6.1 Limitations

The proposed model comes with several limitations and avenues for further development. First, it assumes a stationary weighting between external and internal influences, whereas this balance may shift over time. Agents could dynamically shift between curiosity-driven exploration of beacons and socially influenced motion following other agents at any point during navigation. Second, our observation model is a first-order dynamical system, where motion trajectories are directly simulated from instantaneous speed. Richer behavioral dynamics may emerge in a second-order formulation that also accounts for acceleration, allowing motion speed to vary during navigation. Both of these extensions would involve time-varying parameters that can be captured in a *superstatistics* framework [74].

Relatedly, our current estimation relied on complete pooling across agents, assuming homogeneous behavior within a group. In more realistic settings, individual differences are expected to play a significant role. Incorporating partial pooling through hierarchical Bayesian modeling can allow us to capture both group and individual-level variability.

And as SBI methods for hierarchical modeling mature [75–77], they can improve the generalizability of ABMs to real-world, heterogeneous behavioral data.

Furthermore, the current model guides agents toward spatial beacons primarily based on proximity, so the intrinsic properties of these beacons could be made more expressive. Future extensions could represent each beacon by a vector of saliency features and each agent by a corresponding vector of saliency modulation states. This would allow agents to approach beacons not only by distance but also by perceived importance, yielding more realistic simulations of interest-driven behavior in the virtual environment. Although our present work focuses exclusively on human motion patterns, the broader goal is to use simulated behavioral dynamics to infer mechanisms of stimulus-driven attention. While known tracking data limit the modeling scope, future developments could incorporate a saliency framework for auditory and visual features [78, 79], and integrate eye-tracking with motion-tracking data to capture the temporal coupling between gaze, head, and body orientation. Such extensions would provide a more complete account of agent response dynamics under various influences.

6.2 Conclusion

We developed a model of human motion dynamics during collective navigation in immersive virtual environments. The model represents agent motion as a mixture of individual and collective influences, and we can use simulation-based inference (SBI) to assess how well the underlying properties of agent locomotion can be recovered from interactions with salient spatial objects in the virtual world. To the best of our knowledge, this work represents one of the first applications of SBI to the study of social dynamics in the built environment. While architecture has only recently emerged as a context for investigating situated human interactions [80], the integration of simulation-based methods into the broader field of human–computer interaction also remains relatively nascent [81].

At the same time, although prior studies have used deep learning to model task-driven multi-agent motion trajectories in finite spatial domains [82], no previous work in virtual environments has modeled the combined influence of local and global factors. By applying SBI in a simulated immersive room, our study takes a first step toward a computational model of distributed cognition in the built environment, with potential applications to human-centered interfaces in intelligent building systems. In doing so, we aim to contribute to the growing development of immersive rooms and other smart environments that can incorporate models of human behavior and ultimately transform how people experience the virtual world together.

Acknowledgement

MJH and STR are supported by the National Science Foundation under Grant No. 2448380. We would like to acknowledge the Collaborative-Research Augmented Immersive Virtual Environment (CRAIVE-Lab) and the Curtis R. Priem Experimental Media and Performing Art Center (EMPAC) at Rensselaer Polytechnic Institute for the facility support of this work. In addition, we would like to acknowledge Ted Krueger, Carla Leitão, and Jonas Braasch for their thoughtful feedback during the development process.

Conflict of Interest Statement

The authors declare no conflict of interest.

Code Availability

The code implementation of the present work can be found in the following GitHub repository: <https://github.com/jerrymhuang/TogetherFlow>.

References

- [1] C. Cruz-Neira, D. J. Sandin, T. A. DeFanti, R. V. Kenyon, and J. C. Hart, “The cave: Audio visual experience automatic virtual environment,” *Commun. ACM*, vol. 35, p. 64–72, 6 1992.
- [2] G. Sharma, J. Braasch, and R. J. Radke, “Interactions in a human-scale immersive environment: The craive-lab,” in *Cross-Surface 2016, in conjunction with the ACM International Conference on Interactive Surfaces and Spaces*, 2017.
- [3] M. Huang, S. R. V. Chabot, C. Leitão, T. Krueger, and J. Braasch, “Spatially-aware group interaction design framework for collaborative room-oriented immersive systems,” *Applied Ergonomics*, vol. 113, p. 104076, 2023.

- [4] J. Kuchera-Morin, M. Wright, G. Wakefield, C. Roberts, D. Adderton, B. Sajadi, T. Höllerer, and A. Majumder, “Immersive full-surround multi-user system design,” *Computers & Graphics*, vol. 40, pp. 10–21, 2014.
- [5] W. Chen, *Collaboration in Multi-user Immersive Virtual Environment*. PhD thesis, Université Paris Saclay (COmUE), 2015.
- [6] T. W. Kuhlen and B. Hentschel, “Quo vadis cave: does immersive visualization still matter?,” *IEEE computer graphics and applications*, vol. 34, no. 5, pp. 14–21, 2014.
- [7] S. Chabot, J. Drozdzal, M. Peveler, Y. Zhou, H. Su, and J. Braasch, “A collaborative, immersive language learning environment using augmented panoramic imagery,” in *2020 6th international conference of the immersive learning research network (iLRN)*, pp. 225–229, IEEE, 2020.
- [8] B. Jones, R. Sodhi, M. Murdock, R. Mehra, H. Benko, A. Wilson, E. Ofek, B. MacIntyre, N. Raghuvanshi, and L. Shapira, “Roomalive: Magical experiences enabled by scalable, adaptive projector-camera units,” in *UIST ’14 Proceedings of the 27th annual ACM symposium on User interface software and technology*, pp. 637–644, ACM, October 2014.
- [9] T. Pejsa, J. Kantor, H. Benko, E. Ofek, and A. Wilson, “Room2room: Enabling life-size telepresence in a projected augmented reality environment,” in *CSCW ’16 Proceedings of the 19th ACM Conference on Computer-Supported Cooperative Work and Social Computing*, pp. 1716–1725, ACM, 2 2016.
- [10] F. A. Sanz, A.-H. Olivier, G. Bruder, J. Pettré, and A. Lécuyer, “Virtual proxemics: Locomotion in the presence of obstacles in large immersive projection environments,” in *2015 IEEE Virtual Reality (VR)*, pp. 75–80, 2015.
- [11] W. H. Warren, J. B. Faladays, K. Yoshida, T. D. Wirth, and B. A. Free, “Human crowds as social networks: Collective dynamics of consensus and polarization,” *Perspectives on Psychological Science*, vol. 19, no. 2, pp. 522–537, 2024. PMID: 37526132.
- [12] D. Kirsh, “Do architects and designers think about interactivity differently?,” *ACM Transactions on Computer-Human Interaction (TOCHI)*, vol. 26, no. 2, pp. 1–43, 2019.
- [13] D. Kirsh, “Reimagining space: how activity space explains human behaviour in buildings,” *Architectural Science Review*, pp. 1–11, 2025.
- [14] R. D. Beer, “Dynamical approaches to cognitive science,” *Trends in Cognitive Sciences*, vol. 4, no. 3, pp. 91–99, 2000.
- [15] E. Bonabeau, “Agent-based modeling: Methods and techniques for simulating human systems,” *Proceedings of the national academy of sciences*, vol. 99, no. suppl_3, pp. 7280–7287, 2002.
- [16] S. De Marchi and S. E. Page, “Agent-based models,” *Annual Review of political science*, vol. 17, no. 1, pp. 1–20, 2014.
- [17] E. Dignum, H. Choudhary, and M. Lees, “Simulation-based inference in agent-based models using spatio-temporal summary statistics,” in *International Conference on Computational Science*, pp. 239–254, Springer, 2025.
- [18] A. Lavin, H. Zenil, B. Paige, et al., “Simulation intelligence: Towards a new generation of scientific methods,” *arXiv preprint*, 2021.
- [19] K. Cranmer, J. Brehmer, and G. Louppe, “The frontier of simulation-based inference,” *Proceedings of the National Academy of Sciences*, 2020.
- [20] S. T. Radev, M. Schmitt, L. Schumacher, L. Elsemüller, V. Pratz, Y. Schälte, U. Köthe, and P.-C. Bürkner, “BayesFlow: Amortized Bayesian Workflows With Neural Networks,” *Journal of Open Source Software*, 2023.
- [21] R. Ratcliff, P. L. Smith, S. D. Brown, and G. McKoon, “Diffusion decision model: Current issues and history,” *Trends in cognitive sciences*, vol. 20, no. 4, pp. 260–281, 2016.
- [22] W. H. Warren, “Collective motion in human crowds,” *Current directions in psychological science*, vol. 27, no. 4, pp. 232–240, 2018.
- [23] J. Bill, S. J. Gershman, and J. Drugowitsch, “Visual motion perception as online hierarchical inference,” *Nature communications*, vol. 13, no. 1, p. 7403, 2022.
- [24] T. Vicsek, A. Czirók, E. Ben-Jacob, I. Cohen, and O. Shochet, “Novel type of phase transition in a system of self-driven particles,” *Phys. Rev. Lett.*, vol. 75, pp. 1226–1229, Aug 1995.
- [25] C. Bechinger, R. Di Leonardo, H. Löwen, C. Reichhardt, G. Volpe, and G. Volpe, “Active particles in complex and crowded environments,” *Rev. Mod. Phys.*, vol. 88, p. 045006, Nov 2016.
- [26] C. W. Reynolds, “Flocks, herds and schools: A distributed behavioral model,” *SIGGRAPH Comput. Graph.*, vol. 21, p. 25–34, aug 1987.

- [27] W. Yan and Y. E. Kalay, “Geometric, Cognitive and Behavioral Modeling of Environmental Users,” in *Design Computing and Cognition '06* (J. S. Gero, ed.), (Dordrecht), pp. 61–79, Springer Netherlands, 2006.
- [28] G. C. Dachner, T. D. Wirth, E. Richmond, and W. H. Warren, “The visual coupling between neighbours explains local interactions underlying human ‘flocking’,” *Proceedings of the Royal Society B*, vol. 289, no. 1970, p. 20212089, 2022.
- [29] G. C. Dachner and W. H. Warren, “Behavioral dynamics of heading alignment in pedestrian following,” *Transportation Research Procedia*, vol. 2, pp. 69–76, 2014.
- [30] T. D. Wirth, G. C. Dachner, K. W. Rio, and W. H. Warren, “Is the neighborhood of interaction in human crowds metric, topological, or visual?,” *PNAS Nexus*, vol. 2, p. 118, May 2023.
- [31] J. Toner, “Why walking is easier than pointing: Hydrodynamics of dry active matter,” *arXiv preprint arXiv:1812.00310*, 2018.
- [32] W. H. Warren, “The dynamics of perception and action.,” *Psychological review*, vol. 113, no. 2, p. 358, 2006.
- [33] D. di Nocera, A. Finzi, S. Rossi, and M. Staffa, “The role of intrinsic motivations in attention allocation and shifting,” *Frontiers in Psychology*, vol. 5, 2014.
- [34] R. A. Abrams and S. E. Christ, “Motion onset captures attention,” *Psychological Science*, vol. 14, no. 5, pp. 427–432, 2003. PMID: 12930472.
- [35] S. L. Prime and L. R. Harris, “Predicting the position of moving audiovisual stimuli,” *Experimental Brain Research*, vol. 203, pp. 249–260, June 2010.
- [36] S. Carlile and J. Leung, “The perception of auditory motion,” *Trends in Hearing*, vol. 20, p. 2331216516644254, 2016.
- [37] J. Leung, V. Wei, M. Burgess, and S. Carlile, “Head tracking of auditory, visual, and audio-visual targets,” *Frontiers in neuroscience*, vol. 9, p. 493, 2016.
- [38] C. S. Royden and E. C. Hildreth, “Human heading judgments in the presence of moving objects,” *Perception & Psychophysics*, vol. 58, pp. 836–856, Jan. 1996.
- [39] V. Roggerone, J. Vacher, C. Tarlao, and C. Guastavino, “Auditory motion perception emerges from successive sound localizations integrated over time,” *Scientific Reports*, vol. 9, no. 1, p. 16437, 2019.
- [40] B. Cohen-Lhyver, S. Argentieri, and B. Gas, “Audition as a trigger of head movements,” in *The Technology of Binaural Understanding* (J. Blauert and J. Braasch, eds.), pp. 697–731, Cham: Springer International Publishing, 2020.
- [41] A. J. Kolarik, B. C. J. Moore, P. Zahorik, S. Cirstea, and S. Pardhan, “Auditory distance perception in humans: a review of cues, development, neuronal bases, and effects of sensory loss,” *Attention, Perception, & Psychophysics*, vol. 78, no. 2, pp. 373–395, 2016.
- [42] M. E. L. Pelley, C. J. Mitchell, T. Beesley, D. N. George, and A. J. Wills, “Attention and associative learning in humans: An integrative review.,” *Psychological bulletin*, vol. 142 10, pp. 1111–1140, 2016.
- [43] R. Fendrich and P. M. Corballis, “The temporal cross-capture of audition and vision,” *Perception & Psychophysics*, vol. 63, pp. 719–725, 5 2001.
- [44] R. Ratcliff and G. McKoon, “The diffusion decision model: theory and data for two-choice decision tasks,” *Neural computation*, vol. 20, no. 4, pp. 873–922, 2008.
- [45] J. Marienhagen, L. B. Moyse, A. Schakowski, B. Kahl, J. Davidson, A. El Hady, R. H. Kurvers, and D. Deffner, “Bridging reinforcement-learning and drift-diffusion modeling to uncover the cognitive processes underlying collective foraging,” *PsyArXiv*, 2025.
- [46] J. Grazzini, M. G. Richiardi, and M. Tsionas, “Bayesian estimation of agent-based models,” *Journal of Economic Dynamics and Control*, vol. 77, pp. 26–47, 2017.
- [47] T. Shiono, “Estimation of agent-based models using Bayesian deep learning approach of BayesFlow,” *Journal of Economic Dynamics and Control*, vol. 125, p. 104082, 2021.
- [48] J. Dyer, P. Cannon, J. D. Farmer, and S. M. Schmon, “Black-box bayesian inference for agent-based models,” *Journal of Economic Dynamics and Control*, vol. 161, p. 104827, 2024.
- [49] M. Youngblood and S. Passmore, “Simulation-based inference with deep learning shows speed climbers combine innovation and copying to improve performance,” *PsyArXiv*, Dec 2024.
- [50] J. Pitocchelli, A. Albina, R. A. Bentley, D. Guerra, and M. Youngblood, “Temporal stability in songs across the breeding range of *geothlypis philadelphia* (mourning warbler) may be due to learning fidelity and transmission biases,” *Ornithology*, p. ukae046, 2024.

- [51] C. Angione, E. Silverman, and E. Yaneske, “Using machine learning as a surrogate model for agent-based simulations,” *PLOS ONE*, vol. 17, pp. 1–24, 02 2022.
- [52] J. Dyer, P. Cannon, and S. M. Schmon, “Approximate bayesian computation with path signatures,” *arXiv preprint arXiv:2106.12555*, 2021.
- [53] A. J. Daly, L. De Visscher, J. M. Baetens, and B. De Baets, “Quo vadis, agent-based modelling tools?,” *Environmental Modelling and Software*, vol. 157, p. 105514, 2022.
- [54] N. Said, M. Engelhart, C. Kirches, S. Körkel, and D. V. Holt, “Applying mathematical optimization methods to an act-r instance-based learning model,” *PloS one*, vol. 11, no. 7, p. e0158832, 2016.
- [55] S. T. Radev, U. K. Mertens, A. Voss, L. Ardizzone, and U. Köthe, “BayesFlow: Learning complex stochastic models with invertible neural networks,” *IEEE transactions on neural networks and learning systems*, 2020.
- [56] M. Sainsbury-Dale, A. Zammit-Mangion, and R. Huser, “Likelihood-free parameter estimation with neural bayes estimators,” *The American Statistician*, vol. 78, no. 1, pp. 1–14, 2024.
- [57] L. Elsemüller, M. Schnuerch, P.-C. Bürkner, and S. T. Radev, “A deep learning method for comparing bayesian hierarchical models.,” *Psychological Methods*, 2024.
- [58] G. D. Clemenson, A. Maselli, A. Fiannaca, A. Miller, and M. Gonzalez Franco, “Rethinking GPS navigation: creating cognitive maps through auditory clues,” *Scientific Reports*, vol. 11, pp. 7764–7764, April 2021.
- [59] M. J. Huang and J. Braasch, “Integrated digital twin of immersive rooms for remote spatial telepresence in shared virtual worlds,” *The Journal of the Acoustical Society of America*, vol. 156, 2024.
- [60] J. G. Neuhoff, “Adaptive biases in visual and auditory looming perception.,” in *Spatial biases in perception and cognition.*, pp. 180–190, New York, NY, US: Cambridge University Press, 2018.
- [61] M. Hayhoe and D. Ballard, “Eye movements in natural behavior,” *Trends in cognitive sciences*, vol. 9, no. 4, pp. 188–194, 2005.
- [62] A. J. Berkhou, D. de Vries, and P. Vogel, “Acoustic control by wave field synthesis,” *The Journal of the Acoustical Society of America*, vol. 93, no. 5, pp. 2764–2778, 1993.
- [63] A. Gelman, J. B. Carlin, H. S. Stern, D. B. Dunson, A. Vehtari, and D. B. Rubin, *Bayesian Data Analysis (3rd Edition)*. Chapman and Hall/CRC, 2013.
- [64] Y. Lipman, R. T. Q. Chen, H. Ben-Hamu, M. Nickel, and M. Le, “Flow matching for generative modeling,” in *The 11th International Conference on Learning Representations*, 2023.
- [65] S. Talts, M. Betancourt, D. Simpson, A. Vehtari, and A. Gelman, “Validating Bayesian inference algorithms with simulation-based calibration,” *arXiv preprint*, 2018.
- [66] T. Säilynoja, P.-C. Bürkner, and A. Vehtari, “Graphical test for discrete uniformity and its applications in goodness-of-fit evaluation and multiple sample comparison,” *Statistics and Computing*, vol. 32, 3 2022.
- [67] Y. Yao and J. Domke, “Discriminative calibration: Check bayesian computation from simulations and flexible classifier,” *Advances in Neural Information Processing Systems*, vol. 36, pp. 36106–36131, 2023.
- [68] D. J. Schad, M. Betancourt, and S. Vasishth, “Toward a principled bayesian workflow in cognitive science.,” *Psychological methods*, vol. 26, no. 1, p. 103, 2021.
- [69] J.-M. Lueckmann, J. Boelts, D. Greenberg, P. Goncalves, and J. Macke, “Benchmarking simulation-based inference,” in *Proceedings of The 24th International Conference on Artificial Intelligence and Statistics* (A. Banerjee and K. Fukumizu, eds.), vol. 130 of *Proceedings of Machine Learning Research*, pp. 343–351, PMLR, 13–15 Apr 2021.
- [70] A. Gelman, A. Vehtari, D. Simpson, *et al.*, “Bayesian workflow,” *arXiv preprint*, 2020.
- [71] H. Wierstorf, A. Raake, and S. Spors, “Assessing localization accuracy in sound field synthesis,” *The Journal of the Acoustical Society of America*, vol. 141, no. 2, pp. 1111–1119, 2017.
- [72] B. Kahl, “Assessing the viability of wave field synthesis in vr-based cognitive research,” *arXiv preprint arXiv:2507.03797*, 2025.
- [73] S. R. Mathias, “Unified analysis of accuracy and reaction times via models of decision making,” in *Proceedings of Meetings on Acoustics*, vol. 26, AIP Publishing, 2016.
- [74] L. Schumacher, M. Schnuerch, A. Voss, and S. T. Radev, “Validation and comparison of non-stationary cognitive models: A diffusion model application,” *Computational Brain & Behavior*, vol. 8, no. 2, pp. 191–210, 2025.

- [75] J. Arruda, Y. Schälte, C. Peiter, O. Teplytska, U. Jaehde, and J. Hasenauer, “An amortized approach to non-linear mixed-effects modeling based on neural posterior estimation,” in *International Conference on Machine Learning*, pp. 1865–1901, PMLR, 2024.
- [76] L. Heinrich, S. Mishra-Sharma, C. Pollard, and P. Windischhofer, “Hierarchical neural simulation-based inference over event ensembles,” *Transactions on Machine Learning Research*, 2024.
- [77] D. Habermann, M. Schmitt, L. Kühmichel, A. Bulling, S. T. Radev, and P.-C. Bürkner, “Amortized bayesian multilevel models,” *arXiv preprint arXiv:2408.13230*, 2024.
- [78] S. Onat, K. Libertus, and P. König, “Integrating audiovisual information for the control of overt attention,” *Journal of Vision*, vol. 7, pp. 11–11, July 2007.
- [79] E. M. Kaya and M. Elhilali, “Modelling auditory attention,” *Philosophical Transactions of the Royal Society B: Biological Sciences*, vol. 372, no. 1714, p. 20160101, 2017.
- [80] H. S. Alavi, E. F. Churchill, M. Wiberg, D. Lalanne, P. Dalsgaard, A. Fatah gen Schieck, and Y. Rogers, “Introduction to human-building interaction (hbi): Interfacing hci with architecture and urban design,” *ACM Trans. Comput.-Hum. Interact.*, vol. 26, Mar. 2019.
- [81] R. Murray-Smith, A. Oulasvirta, A. Howes, J. Müller, A. Ikkala, M. Bachinski, A. Fleig, F. Fischer, and M. Klar, “What simulation can do for hci research,” *Interactions*, vol. 29, p. 48–53, Nov. 2022.
- [82] S. Omidshafiei, D. Hennes, M. Garnelo, E. Tarassov, Z. Wang, R. Elie, J. T. Connor, P. Muller, I. Graham, W. Spearman, *et al.*, “Time-series imputation of temporally-occluded multiagent trajectories,” *arXiv preprint arXiv:2106.04219*, 2021.